ReneSANCe event generator for precision e^+e^- physics

Renat Sadykov
(JINR, Dubna)
on behalf of SANC group

Joint Workshop of the CEPC Physics, Software and New Detector Concept
16.04.2021, YangZhou

Outline

- Review of SANC products for e^+e^-
- ReneSANCe Monte Carlo generator
- Results for implemented processes at NLO EW
  - $e^+e^- \to e^+e^-$
  - $e^+e^- \to ZH$
  - $e^+e^- \to \mu^+\mu^-, \tau^+\tau^-$
- Higher order corrections
- Summary and plans

The SANC framework and products family

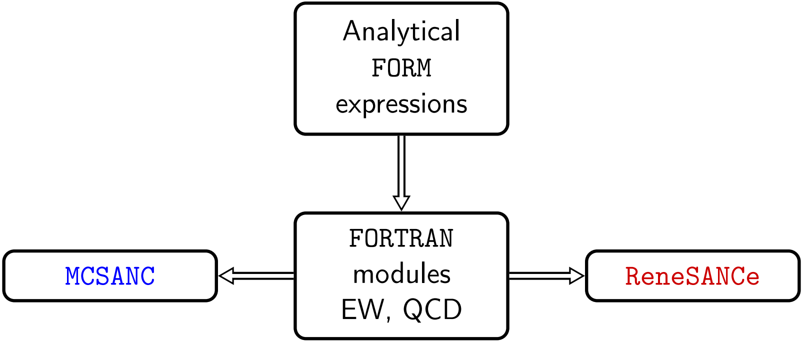

Publications:

SANC – Comput.Phys.Commun. 174 (2006), 481-517.
MCSANC (pp-mode) – Comput.Phys.Commun. 184 (2013), 2343-2350; JETP Letters 103 (2016), 131-136.
ReneSANCe – Comput.Phys.Commun. 256 (2020), 107445.

SANC products are available at http://sanc.jinr.ru/download.php

ReneSANCe **generator**

ReneSANCe (Renewed SANC Monte Carlo event generator) is a Monte Carlo event generator for simulation of processes at e^+e^- colliders.

- The following processes are fully implemented:
  - Bhabha scattering ($e^+e^- \to e^-e^+$)
  - Higgs-strahlung ($e^+e^- \to ZH$)
  - s-channel ($e^+e^- \to \mu^+\mu^-, \tau^+\tau^-$)
- Based on the SANC (Support for Analytic and Numeric Calculations for experiments at colliders) modules
- Complete one-loop and some higher-order electroweak radiative corrections
- All the particle masses and polarizations
- Effectively operates in the collinear region and in wide $\sqrt{s}$ range
- New processes can be easily added

Scheme of FF calculations

The calculations are organized in a way to control consistency of result.

- All calculations at the one-loop precision level are realized in the R_ξ gauge with three gauge parameters: ξ_{A}, ξ_{Z} and $\xi \equiv \xi_{\mathrm{W}}$
- To parameterize ultraviolet divergences, dimensional regularization is used
- Loop integrals are expressed in terms of standard scalar Passarino-Veltman functions: $A_0,\ B_0,\ C_0,\ D_0$

These features make it possible to carry out several important checks at the level of analytical expressions, e.g., checking the gauge invariance by eliminating the dependence on the gauge parameter, checking cancellation of ultraviolet poles, as well as checking various symmetry properties and the Ward identities.

Cross section structure at one-loop

The cross-section of processes at one-loop can be devided into four parts:

$$\sigma^{\text{1-loop}} = \sigma^{\text{Born}} + \sigma^{\text{virt}}(\lambda) + \sigma^{\text{soft}}(\lambda, \omega) + \sigma^{\text{hard}}(\omega),$$

where

σ^{Born} — Born level cross section,
σ^{virt} — virtual (loop) corrections,
σ^{soft} — soft photon bremsstrahlung,
σ^{hard} — hard photon bremsstrahlung (with energy $E_\gamma > \omega$).
Auxiliary parameters λ ("photon mass") and ω cancel out after summation.

Decomposition of the $e^{\pm}$ polarization vectors

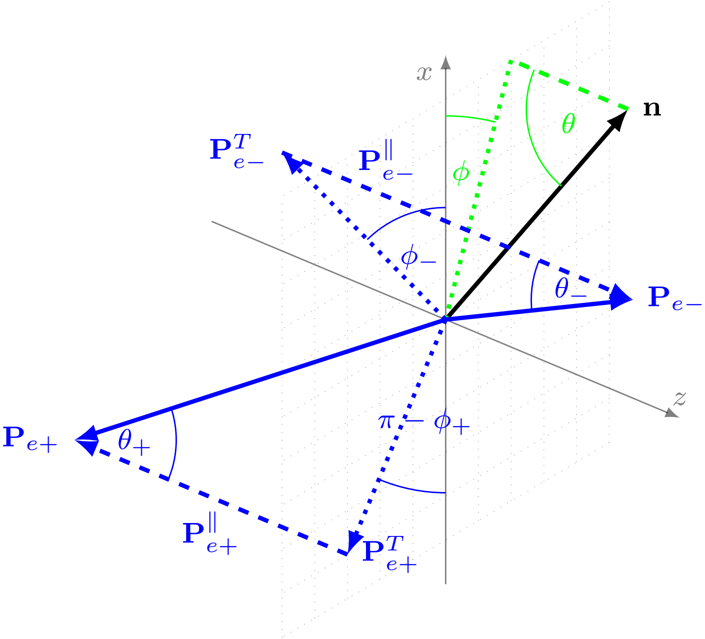

Matrix element squared

$$
\begin{aligned}
|\mathcal{M}|^2 \quad = \quad & L^{\shortparallel}_{e^-} R^{\shortparallel}_{e^+} |\mathcal{H}_{-+}|^2 + R^{\shortparallel}_{e^-} L^{\shortparallel}_{e^+} |\mathcal{H}_{+-}|^2 + L^{\shortparallel}_{e^-} L^{\shortparallel}_{e^+} |\mathcal{H}_{--}|^2 + R^{\shortparallel}_{e^-} R^{\shortparallel}_{e^+} |\mathcal{H}_{++}|^2 \\
& - \frac{1}{2} P^{\perp}_{e^-} P^{\perp}_{e^+} Re\left[e^{i(\Phi_+ - \Phi_-)} \mathcal{H}_{++} \mathcal{H}^*_{--} + e^{i(\Phi_+ + \Phi_-)} \mathcal{H}_{+-} \mathcal{H}^*_{-+} \right] \\
& + P^{\perp}_{e^-} Re\left[e^{i\Phi_-} \left(L^{\shortparallel}_{e^+} \mathcal{H}_{+-} \mathcal{H}^*_{--} + R^{\shortparallel}_{e^+} \mathcal{H}_{++} \mathcal{H}^*_{-+} \right) \right] \\
& - P^{\perp}_{e^+} Re\left[e^{i\Phi_+} \left(L^{\shortparallel}_{e^-} \mathcal{H}_{-+} \mathcal{H}^*_{--} + R^{\shortparallel}_{e^-} \mathcal{H}_{++} \mathcal{H}^*_{+-} \right) \right],
\end{aligned}
$$

where

$$
L^{\shortparallel}_{e^\pm} = \frac{1}{2}(1 - P^{\shortparallel}_{e^\pm}), \quad R^{\shortparallel}_{e^\pm} = \frac{1}{2}(1 + P^{\shortparallel}_{e^\pm}), \quad \Phi_\pm = \phi_\pm - \phi,
$$

$\mathcal{H}_{--}$, $\mathcal{H}_{++}$, $\mathcal{H}_{-+}$, $\mathcal{H}_{+-}$ — helicity amplitudes.

Moortgat-Pick, G. et al. Phys.Rept. 460 (2008) 131-243

Helicity approach

We use the helicity approach for all contributions.
It provides us possibility to describe in the future:

- any initial (not only longitudinal) polarization
- polarization of final states
- spin correlations, polarization transfer from initial to final states

ReneSANCe **generator**

- CMAKE build system
- Modular architecture
- c++ & FORTRAN
- For sampling we used adaptive algorithm mFOAM
  Jadach, S. and Sawicki, P., Comp. Phys. Comm. 177 (2007), pp. 441–458

ReneSANCe **code structure**

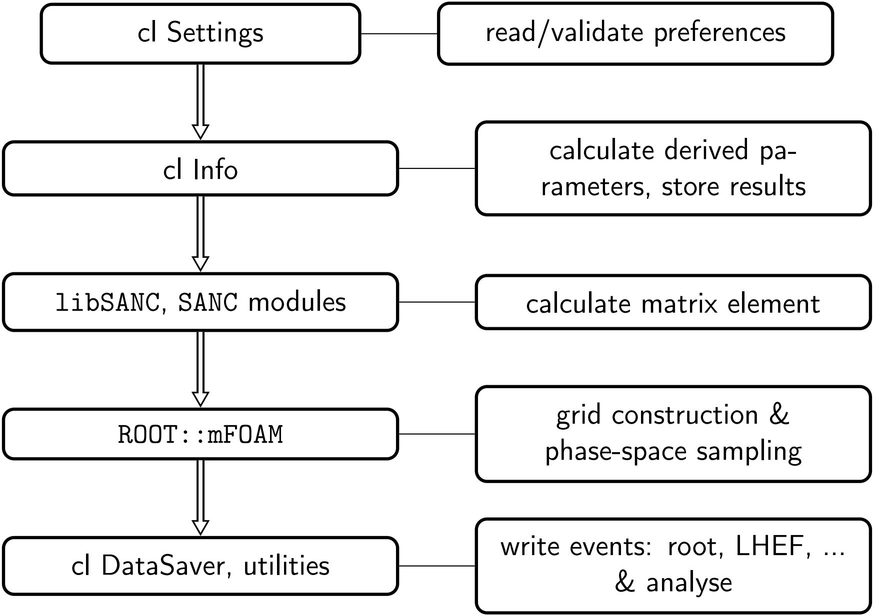

ReneSANCe **settings**

```
schema: {
properties: {
#!!!!!!!!!!!!!!!!!!!!!!!!!!!!!!!!!!!!!!!!!!!!!!!!!!!!!!!!!!!!!!!!!!
# Process id:
pid : {type: integer, minimum: 101, maximum: 104}
    # 101 - e^+e^-  --> e^-e^+
    # 102 - e^+e^-  --> ZH
    # 103 - e^+e^-  --> mu^-mu^+
    # 104 - e^+e^-  --> tau^-tau^+
#!!!!!!!!!!!!!!!!!!!!!!!!!!!!!!!!!!!!!!!!!!!!!!!!!!!!!!!!!!!!!!!!!
# ALR:
alr  : {type: integer, minimum: 0, maximum: 4, default: 0}
    # 0 - sigma, 1 - sigma_RL-sigma_LR, 2 - sigma_RL+sigma_LR,
    # 3 - sigma_0L-sigma_0R, 4 - sigma_0L+sigma_0R
```

```
#!!!!!!!!!!!!!!!!!!!!!!!!!!!!!!!!!!!!!!!!!!!!!!!!!!!!!!!!!!!!!!!!!!
# Process id:
pid : 101
    # 101 - e^+e^-  --> e^-e^+
    # 102 - e^+e^-  --> ZH
    # 103 - e^+e^-  --> mu^-mu^+
    # 104 - e^+e^-  --> tau^-tau^+
#!!!!!!!!!!!!!!!!!!!!!!!!!!!!!!!!!!!!!!!!!!!!!!!!!!!!!!!!!!!!!!!!!!
# ALR:
alr  : 0
    # 0 - sigma, 1 - sigma_RL-sigma_LR, 2 - sigma_RL+sigm
```

```
Validation of 'pid'='108' failed:
'number is too big: 108.000, maximum is: 107.000'
Requirements:
type = "integer";
minimum = 101;
maximum = 107;
```

Sampling strategy

For sampling we used a multibranching strategy with variable transformation. We implemented two approaches.

- Manual sampling over branches. For each branch, we created a separate instance of the `FOAM` class. In this case, each branch can use both optimal variable transformation and the optimal `FOAM` setup. As a consequence, an additional stage is needed to calculate branching weights that slow down the initialization stage of the generator.
- Sampling is made using only one instance of the `FOAM`. Nevertheless, optimal variable transformation for each branch is also available. The `FOAM` is responsible for sampling over branching. It is performed by creating additional artificial dimension of integral with fixed division points.

Basic processes of SM for e^+e^- annihilation

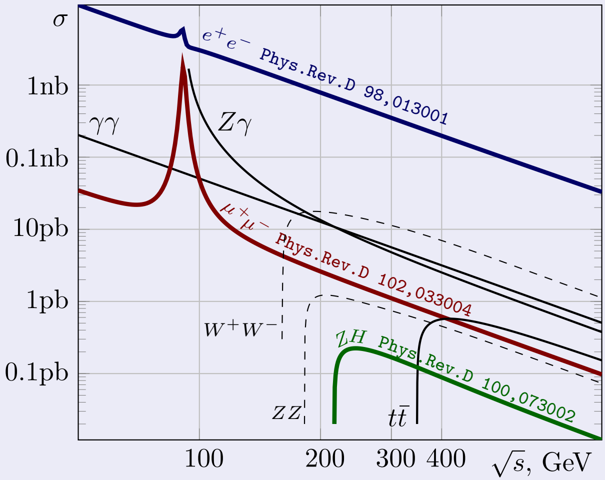

The cross sections are given for polar angles between $10^o < \theta < 170^o$ in the final state.

Numerical results: Setup for tuned comparison

$$
\begin{aligned}
\alpha^{-1}(0) &= 137.03599976, & M_W &= 80.451495 \text{ GeV}, & \Gamma_W &= 2.0836 \text{ GeV},\\
M_H &= 125.0 \text{ GeV}, & M_Z &= 91.1867 \text{ GeV}, & \Gamma_Z &= 2.49977 \text{ GeV},\\
m_e &= 0.5109990 \text{ MeV}, & m_\mu &= 0.105658 \text{ GeV}, & m_\tau &= 1.77705 \text{ GeV},\\
m_d &= 0.083 \text{ GeV}, & m_s &= 0.215 \text{ GeV}, & m_b &= 4.7 \text{ GeV},\\
m_u &= 0.062 \text{ GeV}, & m_c &= 1.5 \text{ GeV}, & m_t &= 173.8 \text{ GeV}.
\end{aligned}
$$

with cuts $|\cos\theta| < 0.9$ (for Bhabha process)

We performed a tuned comparison of our results for polarized Born and hard bremsstrahlung with the results `WHIZARD` [Eur.Phys.J.C71 (2011) 1742] and `CalcHEP` [CPC 184(2013) 1729-1769] programs.

Unpolarized Soft + virtual contribution agree with the results of `aI˚TALC` [CPC 174 (2006) 71-82] (for $e^+e^- \to e^+e^-, \mu^+\mu^-, \tau^+\tau^-$) and `Grace-Loop` [Phys.Rept. 430 (2006) 117-209] (for $e^+e^- \to ZH$)

$e^+e^- \to e^-e^+$

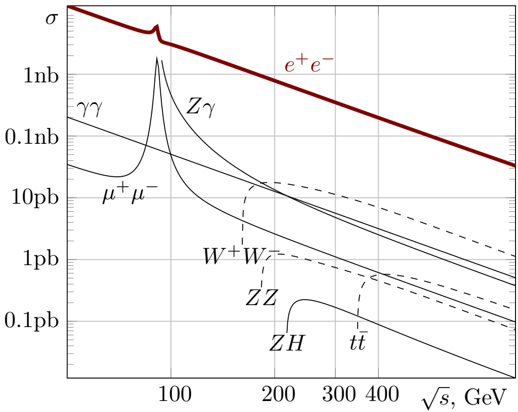

σ
1nb
0.1nb
10pb
1pb
0.1pb
100
200
300
400
√s, GeV
e⁺e⁻
γγ
Zγ
μ⁺μ⁻
W⁺W⁻
ZZ
ZH
tt̄

$e^+e^- \to e^-e^+$

comparison with WHIZARD and CalcHEP for σ^{Born} and σ^{hard} at $\sqrt{s} = 250$ GeV

P_{e^+}	P_{e^-}	ω, $\frac{\sqrt{s}}{2}$	code	σ^{Born}, pb	σ^{hard}, pb	$\sigma^{\text{B+v+s}}$, pb	$\sigma^{\text{1-loop}}$, pb	δ, %
-1	-1	10^{-6}	ReneSANCe	55.263(1)	154.99(1)	$-93.396(1)$	61.60(1)	11.46(1)
		10^{-5}	ReneSANCe		127.65(1)	$-66.063(1)$	61.59(1)	11.45(1)
			WHIZARD	55.264(1)	127.7(1)			
			CalcHEP	55.263(1)	127.6(1)			
-1	1	10^{-6}	ReneSANCe	55.346(1)	152.23(1)	$-92.551(1)$	59.69(1)	7.83(2)
		10^{-5}	ReneSANCe		125.11(1)	$-65.411(1)$	59.71(1)	7.88(2)
			WHIZARD	55.345(1)	124.8(1)			
			CalcHEP	55.346(1)	125.2(1)			
1	-1	10^{-6}	ReneSANCe	60.834(1)	167.56(1)	$-103.633(2)$	63.92(1)	5.08(1)
		10^{-5}	ReneSANCe		137.71(1)	$-73.794(1)$	63.92(1)	5.07(1)
			WHIZARD	60.833(1)	137.6(1)			
			CalcHEP	60.834(1)	137.8(1)			
1	1	10^{-6}	ReneSANCe	55.253(1)	154.99(1)	$-93.396(1)$	61.60(1)	11.46(1)
		10^{-5}	ReneSANCe		127.66(1)	$-66.065(1)$	61.60(1)	11.46(1)
			WHIZARD	55.263(1)	127.7(1)			
			CalcHEP	55.263(1)	127.6(1)			

$e^+e^- \to e^-e^+$

results for 1-loop EW corrections

$\sqrt{s}$	P_{e^+}, P_{e^-}	**0, 0**	0, -0.8	-0.6, -0.8	0.6, -0.8
250 GeV	σ^{Born}, fb	**56.676(1)**	57.774(1)	56.273(1)	59.275(1)
	$\sigma^{\text{1-loop}}$, fb	**61.73(1)**	62.59(1)	61.88(1)	63.29(1)
	δ,%	**8.9(1)**	8.3(1)	10.0(1)	6.8(1)
500 GeV	σ^{Born}, fb	**14.379(1)**	15.030(1)	12.706(1)	17.355(1)
	$\sigma^{\text{1-loop}}$, fb	**15.47(1)**	15.87(1)	13.86(1)	17.88(1)
	δ,%	**7.6(1)**	5.6(1)	9.1(1)	3.1(1)
1000 GeV	σ^{Born}, fb	**3.6792(1)**	3.9057(1)	3.0358(1)	4.7756(1)
	$\sigma^{\text{1-loop}}$, fb	**3.864(1)**	3.945(1)	3.233(1)	4.654(1)
	δ,%	**5.0(1)**	1.0(1)	6.5(1)	$-2.5(1)$

$e^+e^- \to e^-e^+$

left-right asymmetry $A_{LR} = \frac{\sigma_{RL}-\sigma_{LR}}{\sigma_{RL}+\sigma_{LR}}$ in $\cos\theta_{e^+}$

$\sqrt{s} = 250$ GeV

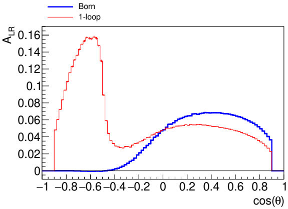

$\sqrt{s} = 500$ GeV

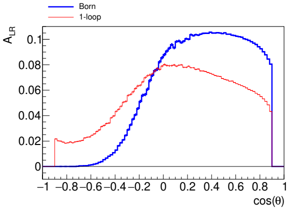

$\sqrt{s} = 1000$ GeV

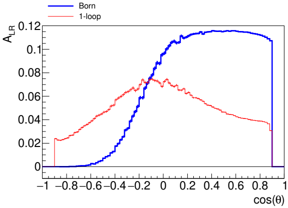

$e^+e^- \to ZH$

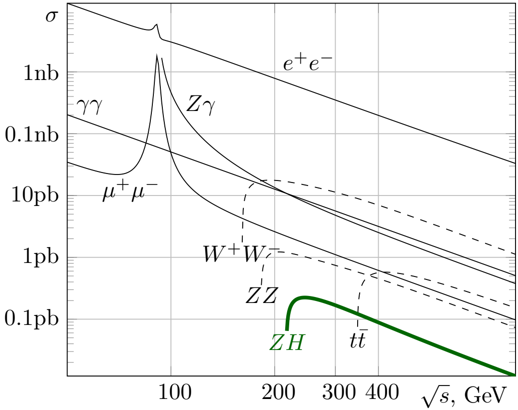

σ
1nb
0.1nb
10pb
1pb
0.1pb
e^+e^-
$\gamma\gamma$
$Z\gamma$
$\mu^+\mu^-$
W^+W^-
ZZ
ZH
$t\bar{t}$
100
200
300
400
$\sqrt{s}$, GeV

$e^+e^- \to ZH$

comparison with WHIZARD and CalcHEP for $\sigma^{\textbf{Born}}$ and $\sigma^{\textbf{hard}}$ at $\sqrt{s} = 250$ GeV

P_{e^+}	P_{e^-}	$\omega,\ \frac{\sqrt{s}}{2}$	code	σ^{Born}, fb	σ^{hard}, fb	$\sigma^{\text{B+v+s}}$, fb	$\sigma^{\text{1-loop}}$, fb	δ, %
-1	-1	0	ReneSANCe	0	0.0260(1)	0	0.0260(1)	—
			WHIZARD	0	0.0259(1)			
			CalcHEP	0	0.0260(1)			
-1	1	10^{-5}	ReneSANCe	350.00(1)	400.85(1)	$-28.82(1)$	372.03(1)	6.30(1)
		10^{-4}			306.51(1)	65.53(1)	372.04(1)	6.30(1)
			WHIZARD	349.99(1)	306.6(2)			
			CalcHEP	350.00(1)	306.5(1)			
1	-1	10^{-5}	ReneSANCe	552.45(1)	632.74(1)	$-177.74(1)$	455.00(1)	$-17.64(1)$
		10^{-4}			483.80(1)	$-28.81(1)$	454.99(1)	$-17.64(1)$
			WHIZARD	552.45(1)	483.7(3)			
			CalcHEP	552.46(1)	483.7(1)			
1	1	0	ReneSANCe	0	0.0260(1)	0	0.0260(1)	—
			WHIZARD	0	0.0260(1)			
			CalcHEP	0	0.0261(1)			

$e^+e^- \to ZH$

results for 1-loop EW corrections

$\sqrt{s}$	P_{e^+}, P_{e^-}	**0, 0**	$0, -0.8$	$-0.6, -0.8$	$0.6, -0.8$
250 GeV	σ^{Born}, fb	**225.59(1)**	266.05(1)	127.42(1)	404.69(1)
	$\sigma^{\text{1-loop}}$, fb	**206.77(1)**	223.33(2)	111.67(2)	339.99(1)
	δ,%	**−8.3(1)**	−16.1(1)	−12.4(1)	−17.2(1)
500 GeV	σ^{Born}, fb	**53.74(1)**	63.38(1)	30.35(1)	96.40(1)
	$\sigma^{\text{1-loop}}$, fb	**62.42(1)**	68.31(1)	34.04(1)	102.58(1)
	δ,%	**16.7(1)**	7.8(1)	12.1(1)	6.4(1)
1000 GeV	σ^{Born}, fb	**12.05(1)**	14.22(1)	6.81(1)	21.62(1)
	$\sigma^{\text{1-loop}}$, fb	**14.56(1)**	15.80(1)	7.95(1)	23.66(1)
	δ,%	**20.8(1)**	11.1(1)	16.7(1)	9.4(1)

$e^+e^- \to ZH$

1-loop EW corrections δ for various polarizations

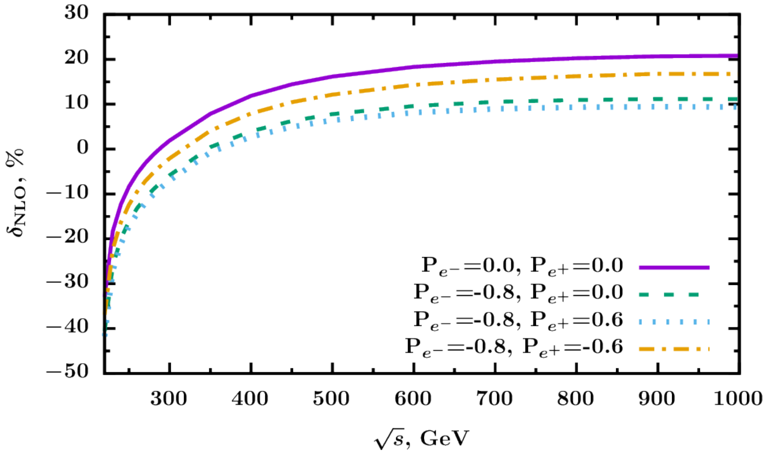

$e^+e^- \to ZH$

1-loop EW corrections δ for different schemes

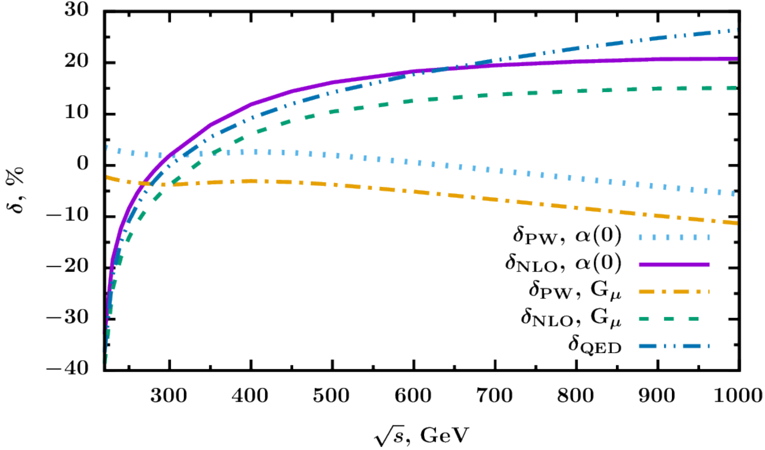

Pure weak (PW) and QED contributions in α_0 and G_μ EW-schemes

$e^+e^- \to ZH$

left-right asymmetry A_{LR} in $\cos\theta_Z$

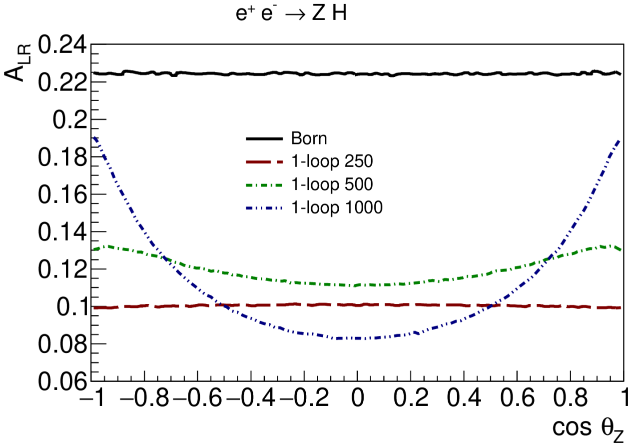

Born and 1-loop for $\sqrt{s} = 250$, 500, 1000 GeV

$$e^+e^- \to \mu^-\mu^+$$
$$e^+e^- \to \tau^-\tau^+$$

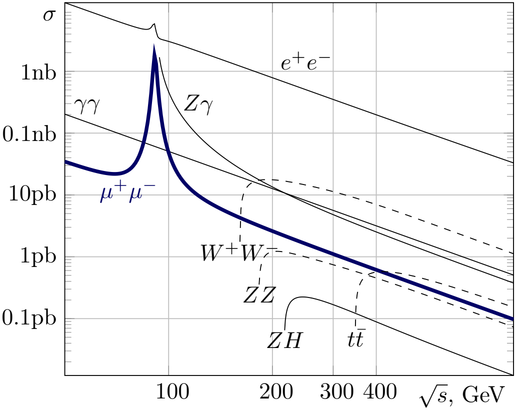

$e^+e^- \to \mu^-\mu^+$

NLO EW results, no cuts

$\sqrt{s}$	P_{e^+}, P_{e^-}	**0, 0**	0, −0.8	0.6, −0.8	−0.6, −0.8
250 GeV	σ^{Born}, fb	**1653.7(1)**	1804.0(1)	2710.5(1)	897.5(1)
	$\sigma^{\text{1-loop}}$, fb	**4526.3(2)**	4915.2(2)	7298.3(4)	2532.0(1)
	δ,%	**173.7(1)**	172.4(1)	169.3(1)	182.1(1)
500 GeV	σ^{Born}, fb	**400.85(1)**	433.51(1)	650.41(1)	216.61(1)
	$\sigma^{\text{1-loop}}$, fb	**1138.9(1)**	1227.7(1)	1818.2(1)	637.2(1)
	δ,%	**184.1(1)**	183.2(1)	179.5(1)	194.2(1)
1000 GeV	σ^{Born}, fb	**99.57(1)**	107.47(1)	161.20(1)	53.75(1)
	$\sigma^{\text{1-loop}}$, fb	**296.70(2)**	318.74(3)	471.61(4)	165.87(1)
	δ,%	**198.0(1)**	196.6(1)	192.6(1)	208.6(1)

$e^+e^- \to \mu^-\mu^+$
NLO EW results with cuts

$\sqrt{s}$	P_{e^+}, P_{e^-}	**0, 0**	0, -0.8	0.6, -0.8	0.6, -0.8
250 GeV	σ^{Born}, fb	**1417.6(1)**	1546.5(1)	2323.5(1)	769.37(2)
	$\sigma^{\text{1-loop}}$, fb	**2399(1)**	2614(1)	3909(1)	1318(1)
	δ,%	**69.2(1)**	69.0(1)	68.2(1)	71.3(1)
500 GeV	σ^{Born}, fb	**343.63(1)**	371.62(1)	557.56(1)	185.69(1)
	$\sigma^{\text{1-loop}}$, fb	**469.8(4)**	495.4(5)	739.3(7)	251.5(2)
	δ,%	**36.7(1)**	33.3(1)	32.6(1)	35.4(1)
1000 GeV	σ^{Born}, fb	**85.355(3)**	92.131(5)	138.18(1)	46.079(2)
	$\sigma^{\text{1-loop}}$, fb	**116.2(1)**	121.1(1)	180.3(1)	61.83(2)
	δ,%	**36.2(1)**	31.4(1)	30.5(1)	34.2(1)

cuts are: $|\cos\theta_{\mu^-}| < 0.9$, $|\cos\theta_{\mu^+}| < 0.9$

$e^+e^- \to \tau^-\tau^+$

SANC vs. WHIZARD (dots): all-polarized

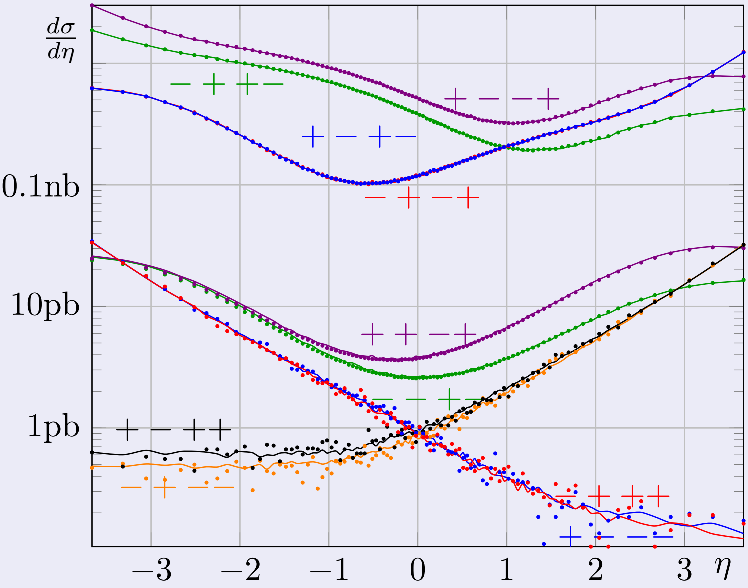

$e^+e^- \to \tau^-\tau^+$

Left–Right Forward–Backward Asymmetry

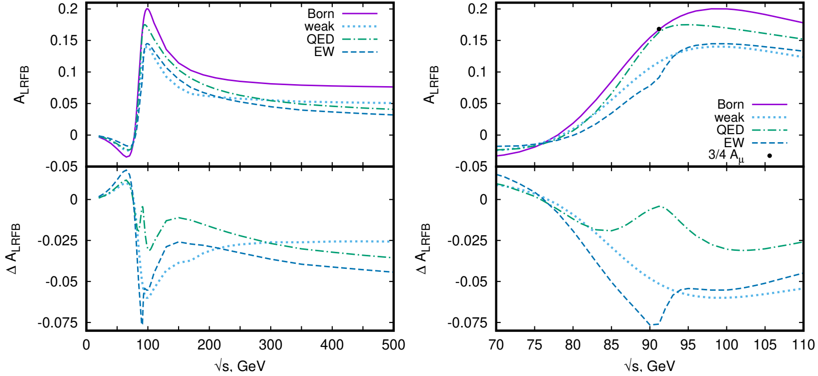

(**Left**) The A_{LRFB} asymmetry in the Born and 1-loop (weak, QED, EW) approximations and ΔA_{LRFB} for c.m.s. energy range; (**Right**) the same for the Z peak region.

$$A_{LRFB} = \frac{(\sigma_{L_e} - \sigma_{R_e})_F - (\sigma_{L_e} - \sigma_{R_e})_B}{(\sigma_{L_e} + \sigma_{R_e})_F + (\sigma_{L_e} + \sigma_{R_e})_B},$$

$e^+e^- \to \tau^-\tau^+$

Final-State Fermion Polarization

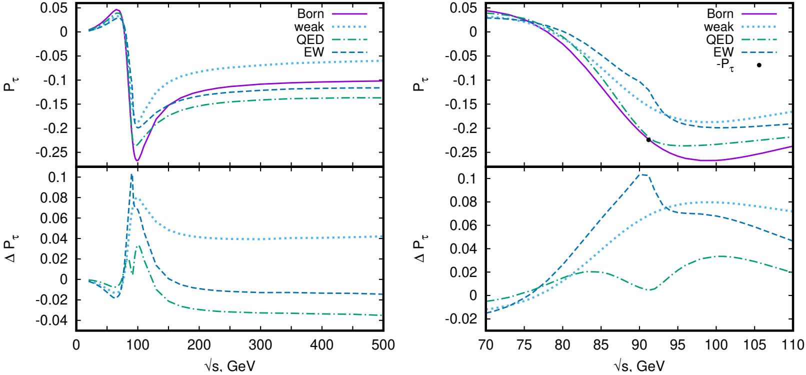

(**Left**) The P_τ polarization in the Born and 1-loop (weak, pure QED, and EW) approximations and ΔP_τ vs. c.m.s. energy in a wide range; (**Right**) the same for the Z peak region. The black dot indicates the Born value P_τ at the Z resonance.

Higher order improvements

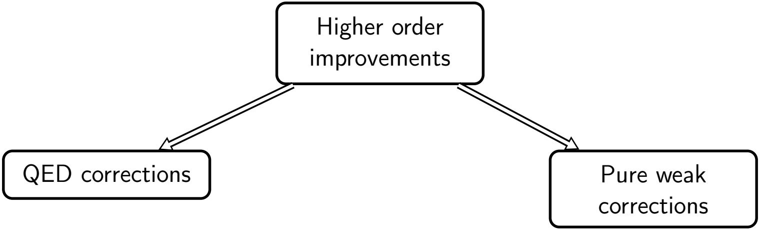

- Leading logarithmic (LL) approximation.
- Corrections to $\Delta\alpha$.
- Shower with matching.

- Corrections to $\Delta\rho$.
- Leading Sudakov logarithms.

Higher order improvements, QED

The leading log in the annihilation channel is $L = \ln \frac{s}{m_l^2}$.

$O(1)$	1		
$O(\alpha)$	αL	α	
$O(\alpha^2)$	$\frac{1}{2}\alpha^2 L^2$	$\frac{1}{2}\alpha^2 L$	$\frac{1}{2}\alpha^2$
$O(\alpha^3)$	$\frac{1}{6}\alpha^3 L^3$	$\frac{1}{6}\alpha^3 L^2$	...

In the LL approximation we can separate pure photonic (marked "γ") and the rest corrections which include pure pair and mixed photon-pair effects (marked as "pair").

$e^+e^- \to \mu^-\mu^+$

ISR corrections in LL approx.

PRELIMINARY

$\sqrt{s} = 250$ GeV, Born cross section $\sigma_0 = 1417.6(1)$ fb.
$\sum \equiv \sum_{n=2}^{4} \mathcal{O}(\alpha^n L^n)$, $\delta = \delta_{\text{ISR LLA}} \equiv \delta\sigma_{\text{ISR LLA}}/\sigma_0$, $\overline{\delta}$ calculated at scale $= 4s$ and $\underline{\delta}$ at scale $= s/4$.

	$\mathcal{O}(\alpha^2L^2)$		$\mathcal{O}(\alpha^3L^3)$		$\mathcal{O}(\alpha^4L^4)$	$\sum$
	$[\gamma]$	[pair]	$[\gamma]$	[pair]	$[\gamma]$	
Cuts: $\lvert\cos\theta_{\mu^\pm}\rvert < 0.9$, $M_{\mu^+\mu^-} > 10$ GeV.						
$\delta\sigma$, fb	108.2(1)	53.70(1)	$-0.49(3)$	3.47(1)	$-0.23(1)$	164.7(1)
δ, %	7.63(1)%	3.79(1)%	$-0.035(2)$%	0.245(1)%	$-0.017(1)$%	11.62(1)%
$\overline{\delta}$, %						13.91(1)%
$\underline{\delta}$, %						11.15(1)%
Cuts: $\lvert\cos\theta_{\mu^\pm}\rvert < 0.9$, $M_{\mu^+\mu^-} > 100$ GeV.						
$\delta\sigma$, fb	4.8(1)	5.9(1)	$-0.76(2)$	0.00(1)	0.00(1)	9.9(1)
δ, %	0.34(1)%	0.42(1)%	$-0.053(1)$%	0.00(1)%	0.00(1)%	0.70(1)%
$\overline{\delta}$, %						0.78(1)%
$\underline{\delta}$, %						0.63(1)%

$e^+e^- \to \mu^-\mu^+$

FSR corrections in LL approx.

PRELIMINARY

$\sqrt{s} = 250$ GeV, Born cross section $\sigma_0 = 1417.6(1)$ fb.
$\sum \equiv \sum_{n=2}^{4} \mathcal{O}(\alpha^n L^n)$, $\delta = \delta_{\text{FSR LLA}} \equiv \delta\sigma_{\text{FSR LLA}}/\sigma_0$, $\bar{\delta}$ calculated at scale $= 4s$ and $\underline{\delta}$ at scale $= s/4$.

	$\mathcal{O}(\alpha^2 L^2)$		$\mathcal{O}(\alpha^3 L^3)$		$\mathcal{O}(\alpha^4 L^4)$	$\sum$
	$[\gamma]$	[pair]	$[\gamma]$	[pair]	$[\gamma]$	
Cuts: $\lvert\cos\theta_{\mu^\pm}\rvert < 0.9$, $M_{\mu^+\mu^-} > 10$ GeV.						
$\delta\sigma$, fb	0.00(1)	7.64(1)	0.00(1)	−0.129(1)	0.00(1)	7.50(1)
δ, %	0.00(1)%	0.539(1)%	0.00(1)%	−0.0091(1)%	0.00(1)%	0.529(1)%
$\bar{\delta}$, %						0.613(1)%
$\underline{\delta}$, %						0.450(1)%
Cuts: $\lvert\cos\theta_{\mu^\pm}\rvert < 0.9$, $M_{\mu^+\mu^-} > 100$ GeV.						
$\delta\sigma$, fb	−0.54(1)	0.87(1)	0.00(1)	−0.069(1)	0.00(1)	0.26(1)
δ, %	−0.038(1)%	0.061(1)%	0.00(1)%	−0.005(1)%	0.00(1)%	0.018(1)%
$\bar{\delta}$, %						0.019(1)%
$\underline{\delta}$, %						0.017(1)%

$e^+e^- \to ZH$

ISR corrections in LL approx.

PRELIMINARY

$\sqrt{s} = 250$ GeV, Born cross section $\sigma_0 = 225.610(1)$ fb.

	$\mathcal{O}(\alpha^2 L^2)\,[\gamma]$	$\mathcal{O}(\alpha^2 L^2)\,\left[e^+e^-\right]$	$\mathcal{O}(\alpha^2 L^2)\,\left[\mu^+\mu^-\right]$	$\mathcal{O}(\alpha^3 L^3)\,[\gamma]$
$\delta\sigma$, fb	$-0.223(1)$	$-0.268(1)$	$-0.159(1)$	$0.211(1)$
δ, %	$-0.099(1)$	$-0.119(1)$	$-0.070(1)$	$0.094(1)$
	$\mathcal{O}(\alpha^3 L^3)\,\left[e^+e^-\right]$	$\mathcal{O}(\alpha^3 L^3)\,\left[\mu^+\mu^-\right]$	$\mathcal{O}(\alpha^4 L^4)\,[\gamma]$	$\sum_{n=2}^{4} \mathcal{O}(\alpha^n L^n)$
$\delta\sigma$, fb	$-0.010(1)$	$-0.006(1)$	$-0.016(1)$	$-0.468(1)$
δ, %	$-0.004(1)$	$-0.003(1)$	$-0.007(1)$	$-0.207(1)$

Higher order improvements, weak

Higher order improvements added through $\Delta\rho$ parameter:
$s_W^2 \to \bar{s}_W^2 \equiv s_W^2 + \Delta\rho\, c_W^2$.

At the two-loop level, the quantity $\Delta\rho$ contains two contributions:

$$\Delta\rho = N_c x_t \left[1 + \rho^{(2)} \left(M_H^2/m_t^2\right) x_t\right] \left[1 - \frac{2\alpha_s(M_Z^2)}{9\pi}(\pi^2 + 3)\right],$$

where $x_t = \frac{\sqrt{2} G_F m_t^2}{16\pi^2}$.

$e^+e^- \to \mu^-\mu^+$

Higher order improvements, weak

PRELIMINARY

P_{e^+}, P_{e^-}	0, 0	0,-0.8	0.3,-0.8	0,0.8	-0.3,0.8
$\sigma^{\mathrm{Born}}_{\alpha(0)}$, pb	1.41763(1)	1.54645(1)	1.93499(1)	1.28880(1)	1.58073(1)
$\sigma^{\mathrm{Born}}_{G_\mu}$, pb	1.50971(1)	1.64690(1)	2.06068(1)	1.37252(1)	1.68341(1)
$\sigma^{\mathrm{Born}}_{\alpha(M_Z^2)}$, pb	1.59923(1)	1.74456(1)	2.18287(1)	1.45391(1)	1.78323(1)
$\delta\sigma^{\mathrm{weak}}_{\alpha(0)}$, pb	0.15525(1)	0.11883(1)	0.14243(1)	0.19167(1)	0.242587(1)
$\delta\sigma^{\mathrm{weak}}_{G_\mu}$, pb	0.07911(1)	0.03249(1)	0.03400(1)	0.12574(1)	0.162206(1)
$\delta\sigma^{\mathrm{weak}}_{\alpha(M_Z^2)}$, pb	-0.01194(1)	-0.07003(1)	-0.09468(1)	0.46147(1)	0.06506(1)
$\delta\sigma^{\mathrm{ho}}_{\alpha(0)}$, pb	0.02122(1)	0.02304(1)	0.02882(1)	0.01940(1)	0.02380(1)
$\delta\sigma^{\mathrm{ho}}_{G_\mu}$, pb	-0.00555(1)	-0.00351(1)	-0.00407(1)	-0.00759(1)	-0.00969(1)
$\delta\sigma^{\mathrm{ho}}_{\alpha(M_Z^2)}$, pb	0.00387(1)	0.00898(1)	0.01183(1)	-0.00124(1)	-0.00222(1)

cuts are: $|\cos\theta_{\mu^-}| < 0.9$, $|\cos\theta_{\mu^+}| < 0.9$.

$e^+e^- \to \mu^-\mu^+$

Impact of various corrections

PRELIMINARY

	Born	+QED (1-loop)	+WEAK (1-loop)	+WEAK ($\Delta\rho$)	+QED (LL)
σ, pb	1.50971(1)	cut1: $+\,0.829(1)$	$+0.07911(1)$	$-0.00555(1)$	cut1: $+\,0.1837(1)$
		cut2: $+\,0.197(1)$			cut2: $+\,0.0108(1)$
$\delta, \%$	100%	cut1: $+\,54.9(1)\%$	$+5.24(1)\%$	$-0.37(1)\%$	cut1: $+\,12.17(1)\%$
		cut2: $+\,13.1(1)\%$			cut2: $+\,0.72(1)\%$

Calculated in G_μ EW scheme, $\sqrt{s} = 250$ GeV.
Cuts are: $|\cos\theta_{\mu^-}| < 0.9$, $|\cos\theta_{\mu^+}| < 0.9$,
cut1: $M_{ll} > 10$ GeV,
cut2: $M_{ll} > 100$ GeV.

Summary

- Monte Carlo event generator ReneSANCe is under development
  - Events with unit weights
  - Initial and final state polarization
  - Complete one-loop EW corrections
  - LL QED and higher order weak corrections through $\Delta\rho$
  - Output in Standard Les Houches Format
  - Simple installation & usage
  - Processes:
    - $e^+e^-, \mu^+\mu^-, \tau^+\tau^-, ZH$ **DONE**
    - $\gamma\gamma, \gamma Z, t\bar{t}$ **UNDERWAY**
  - Plans: new processes, resonance approx., QED showers, EW Sudakov logarithms

ReneSANCe v1.1.1 is available at
http://sanc.jinr.ru/download.php
https://renesance.hepforge.org

Thank you!